CHINESE JOURNAL OF PHYSICS VOL. 24, NO. 4 WINTER 1986

Miissbauer Effect Study of Spin Fluctuation in Some Ferric Oxides*

T.M. Uen (溫增明)
Department of Electrophysics, Chiao-Tung University, Hsin-Chu, Taiwan, 30050

F.H. Yang (楊豐豪)
Department of Physics, Taiwan University, Taipei, Taiwan, 10764

L.F. Chiang (江林富)
Department of Physics, Tamkang University, Tamsui, Taiwan, 25137

H.M. Tsai (蔡惠美)
Institute of Applied Chemistry, Chiao-Tung University, Hsin-Chu, Taiwan, 30050

and

T.Y. Tseng (曾俊元)
Institute of Electronics, Chiao-Tung University, Hsin-Chu, Taiwan, 30050

(Received 8 September 1986)

Mössbauer spectroscopy was used to study the spin fluctuations of the ferric ions at various sites in Ni-Zn ferrites, Y–Al irongamet, and iron-doped β'' -alumina. The temperature dependences of the spin relaxation rates were determined, in particular, near the critical temperature.

J. JNTRODUCTJON

It is often observed that the Mössbauer spectra of many magnetically ordered materials at higher temperatures are characterized by the significant broadening of the Zeeman lines and the growth of inner lines at the expense of outer ones.[1,2] These spectra can not be explained if single–valued static hyperfine fields are assumed. For amorphous ferromagnets, such spectra are generally believed to be mainly due to the distributions of the magnetic hyperfine fields arising from the random arrangments of the atoms. Much valuble information about the microscopic environments of the Mössbauer muclei and about structure

transformations have actually been obtained from successful fitting of the experimental spectra for such systems.* For crystalline magnetic systems, these anomalous Mössbauer spectra are generally recognized to be due to the presence of electronic spin-fluctuation or spin–relaxation.[1,3-8]

The relaxation effect of the electronic spin to the Mossbauer spectrum occurs when the relaxation rate $R=\tau^{-1}$ is comparable with the frequency parameter ω_N A/h which is the characteristic of the hyperfine interaction. Where τ is the lifetime or the correlation time of the electronic level and is related to the matrix element for relaxation. 4 is the hyperfine constant. In the effective hyperfine field approximation a natural choice of ω_N is the nuclear Larmor precession frequency $\omega_L = A/A/\hbar$. The effect of relaxation on the Mössbauer transitions is complex as $R\rightarrow\omega_N$ so that the mathematical expression for the Mossbauer relaxation-lineshape is very complex even when a polarizing field is present or when the hyperfine field approximation is valid.

Relatively few successful fittings to the Mössbauer spectra of a magnetically ordered system by using the relaxation lineshapes have been reported and the information about spin relaxation thus obtained is not very fruitful and rather qualitative. [1,3-8,13,14] In view of of this fact and in view of the importance of the Mossbauer relaxation parameters to the understanding of the dynamical behavior of spins, a Mössbauer–effect study of the spin fluctuation in some magnetic oxides was started in our laboratory. We report here some of our results about Ni-Zn ferrite, Y-Al iron garnet, and iron-doped β''–alumina samples. We will discuss first the Mossbauer relaxation lineshape, then apply it to analyze the spectra of these illustrative systems. The relaxation mechanisms will also be discussed where possible.

JJ. MÖSSBAUER RELAXATJON LJNESHAPES

Numerous theories of the Mössbauer lineshape in the presence of electron spin fluctuation have been published in the past 20 years. However, these theories can be devided into two general categories: the stochastic and the perturbation ones. We will outline both the stochastic and perturbation approaches to the lineshape in the following paragraphs.

A. The Stochastic Approach

In the stochastic approach to the relaxation lineshape, the hyperfine interaction $H_M = AI\cdot S$ between the nuclear spin I and the electron spin S is replaced by an interaction V(t) between the nuclear spin and a randomly varying external magnetic field $H_{ext}(t)$.

$$V(t) = AI_z S_z(t) = -g_N \mu_N I_z H_{ext}(t). \quad (1)$$

The total Hamiltonian is now written as

$$H = H_o + V(t) \tag{2}$$

Since H_{ext} is proportional to $S_z(t)$, V(t) and H can only have a finite number of forms corresponding to the possible values of S_z. A further assumption is that V(t) and H_o are effectively diagonal in the angular momentum eigenstates. The general expression $I(\omega)$ for the lineshape,

$$I(o) = (1/\Gamma)\mathrm{Re}\int_0^\infty dt\, \exp(i\omega t - \Gamma t) < H^- (0)\ H+(t) > \tag{3}$$

is then calculated by averaging the correlation function $<H^-(0)H^+(t)>$ stochastically. Here Γ is the natural linewidth and H-(t) is the Hermitian adjoint of the electromagnetic interaction H+(t) responsible for the Mdssbauer gamma ray transition in the Heisenberg representation.

For ^{57}Fe the relaxation lineshape is given by [10]

$$I(w) = \sum_{M_g, M_e} I_{M_g M_e}(\omega) \tag{4}$$

with

$$I_{M_g M_e} = (1/\Gamma)\ \mathrm{Re}[\zeta \cdot A^{-1} \cdot \eta]. \tag{5}$$

where M_g and M_e are the eigen values of the angular momentum I_z, ζ is a row vector whose 1 th component is the relative probability that the electronic spin is in its 1 -th state, η is a column vector with all components equal to 1, and A- ' is the inverse of a nxn complex matrix A with n equal to the number of possible electronic spin states. If the electronic transition satisfies the selection rule $\Delta S_z = \pm 1$, then for Fe^{3+} the matrix A is given by [9]

$$A = \begin{vmatrix} i(5\delta-\omega) - 5\Omega_e - \Gamma & 5\Omega_e & 0 & 0 & 0 & 0 \\ 5p\Omega_e & i(3\delta-\omega) - (8+5p)\Omega_e + \Gamma & 8\,\% & 0 & 0 & 0 \\ 0 & 8p\Omega_e & i(\delta-\omega) - (9+8p)\Omega_e + \Gamma & 9\Omega_e & 0 & 0 \\ 0 & 0 & 9p\Omega_e & -i(\delta+\omega) - (8+p)\Omega_e + \Gamma & 8\Omega_e & 0 \\ 0 & 0 & 0 & 8p\Omega_e & -i(3\delta+\omega) - (5+8p)\Omega_e + \Gamma & 5\Omega_e \end{vmatrix} \tag{6}$$

$$\begin{bmatrix} 0 & 0 & 0 & 0 & 5p\Omega_e & -i(5\delta+\omega) \\ & & & & & -5p\Omega_e+\Gamma \end{bmatrix}$$

In the last expression, 10 δ is the separation of the Miissbauer lines corresponding to $S_z=\pm 5/2$ when $\Omega_e=0$,p is the Boltzmann factor for the populations in ionic Zeeman levels. The transition probabilities for $S_z=5/2\rightarrow 3/2, 3/2\rightarrow 1/2, \ldots, -3/2\rightarrow -5/2$ are given respectively by $5\Omega_e, 8\Omega_e, 9\Omega_e, 8\Omega_e, 5\Omega_e$. The electron spin relaxation time τ is related to Ω_e by

$$\tau^{-1} = 7\,(1+p)\Omega_e. \tag{7}$$

An important result of Eqs.(5) and (6) should be particularly mentioned here. When $\Omega_e \rightarrow 0$, these expressions give rise to six sharp Mössbauer peaks at $\omega = +5\delta, +3\delta, \ldots, -56$ with relative intensities given by the vector ζ for each nuclear transition $|M_g\rangle \rightarrow |M_e\rangle$. In this case the positions of peaks are independent of $\langle S_z \rangle$. For high spin flip frequency only one sharp peak occurs at $\omega = 26 < S_z >$ and in this case the position of the peak measures the average spin.

The stochastic model is valid when the electronic part of the hyperfine interaction has no off-diagonal matrix elements, since an external magnetic field has no such elements. Therefore this model is reasonable for a system in which the splitting of electronic levels is large compared with the hyperfiie splitting. If the splitting of electronic levels is not large enough, the off-diagonal matrix elements become important in determining the Mössbauer lineshape. Clauser and Blume have generalized the stochastic model to include this off-diagonal effect." Their expression of the relaxation lineshape involves the inverse of a complex matrix of dimension $(2S+1)^2(2I_g+1)(2I_e+1)$,

Fe^{3+}, this matrix is a 288 **x** 288 complex one.

The stochastic lineshapes (Eq.(6) or other ones) have been applied to explain the relaxation spectra of some paramagnetic materials" and of so'me magnetic ordered systems including neptunium compounds' , K_2FeO_4[8], Co-Zn ferites[12], and Ni-Zn ferrites.[6,13] For these ordered systems, the "best fit" theoretical curves agree satisfactorily with experimental spectra only when the temperates are not very near the critical temperatures.

B. The Perturbation Approach

In the perturbation approach to the relaxation lineshape, one starts with the exact Hamiltonian for the entire system to calculate the correlation function $< H\text{-}(O)\ H^+(t) >$ in Eq.(3). The hyperfme interaction H_M is treated as a peturbation and the time-dependent perturbation expansion method is used.

For the 14.4 KeV magnetic dipole transition of ^{57}Fe, H^+ can be written as[14]

$$H+= \eta \mathbf{I} \cdot \nabla \times A \tag{8}$$

where I is the intrinsic angular momentum operator associated with the nuclear transition,

η is a parameter related to the dipolar strength of the transition, and A is the vector potential of the gamma ray (k, ω). Using this H^+, the expression of the Miissbauer lineshape for the particular nuclear transition $|M_g\rangle$ to $|M_e\rangle$ is given by[14]

$$I_{M_g M_e}(\omega) = \sum_{p=-1}^{+1} G_p(\theta) \int_{-\infty}^{\infty} dt \exp(i\omega t - \Gamma|t|)(-1)^p \cdot \langle I^{-p}(t) I^p(0) \rangle \quad (9)$$

where $G_p(\theta)$ is a geometry factor depending on the angle θ between k and the assumed axis of crystal symmetry. For the magnetically ordered system, it is convenient to write the unperturbed Hamiltonian of the system, when the Mössbauer neucleus is in the excited state, as[15]

$$H_{oe} = H_{elec} + A_e^z I_{ez} \langle S_z \rangle + \hbar\omega_0 \quad (10)$$

and the perturbation as

$$H_e' = \sum_{i=x,y,z} A_e^i I_{ei} (S_i - \delta_{iz} \langle S_z \rangle). \quad (11)$$

In the above equations, H_{elec} is the Hamiltonian of the interacting electron system, and the A_e's are the hyperfine constants. Similar expressions can be written when the nucleus is in the ground state. Based on the assumption that $R >> \omega_N$ in the magnetically ordered system, the correlation function $\langle I^{-p}(t) I^p(0) \rangle$ in Eq.(9) can be expanded and factored into a time independent part involving the nuclear angular momentum operator and a time dependent part involving the spin correlation functions $\phi_i(t)$:

$$\phi_i(t) = \langle \delta S_i(t) \delta S_i(0) \rangle \quad (12)$$

where $\delta S_i(t) = S_i(t) - \langle S_i \rangle$; i = x,y,z. Assuming δS_i is small and the x- and y- directions are equivalent, the longitudinal and transverse correlation functions can be written as[16]

$$\phi_L(t) = \langle (\delta S_z)^2 \rangle \exp(-R_L|t|)$$

$$\phi_T(t) = \langle (\delta S_x)^2 \rangle \exp(-R_T|t|) \quad (13)$$

were R_L and R_T are respectively the longitudinal and transverse relaxation rate, $\langle (\delta S_x)^2 \rangle = \langle S_x^2 \rangle = \langle S_y^2 \rangle$. The lineshape function for the particular Mössbauer transition $|M_g\rangle$ to $|M_e\rangle$ is given by'

$$I_{M_g M_e}(\omega) = \sum_{p=-1}^{+1} |\langle M_g | I^{-p} | M_e \rangle|^2 \cdot \exp(C_L A_{M_g M_e}/R_L^2 + C_T B_{M_g M_e}/R_T^2)$$

$$\cdot \int_{-\infty}^{\infty} \quad [\omega \quad (\omega_g^z M_g - \omega_g^z M_e)]$$

$$+ [-(\Gamma_{M_g M_e} + \mathrm{CLAM}\ M_g\ M_e /R_L + C_T B_{M_g M_e}/R_T)|t|\ 1$$

$$\cdot \exp\ -[/R_L^2)\mathrm{MeM}\ p\ (-R_L\ |t|) + (C\ T\ B\ M\ M_g\ M_e /R_L^2) \exp(-R_L\ |t|)] \quad (14)$$

where: $C_L = <(\delta S_z)^2>$, $C_T = <S_x^2>$, ω_g^z = A, $<S_z>/\hbar$, $\omega_e^z = A_e^z <S_z>/\hbar$, $A_{M_g M_e}$ $= (A_g^z M_g - A_e^z M_e)^2$, $B_{M_g M_e} = (A_g^x)^2 (I_g^2 + I_g^2 - M_g^2) + (A_e^x)^2 (I_e^2 + I_e - M_e^2)$, and $\Gamma_{M_g M_e}$ is

the half-width in the absence of relaxation broadening.

The first line of Eq.(14) relates to the relative intensity of the transition in the presence of ionic spin relaxation. The second line gives the position $\omega_{M_g M_e} = \omega_e^z M_e - \omega_g^z M_g$ of the Mossbauer peak. Note that the line position is now proportional to $<S_z>$, the average of ionic spin. This result originates from the assumption that the relaxation rates are much higher than the hyperfine constants (in frequency unit) for magnetically ordered systems. The third, fourth, and fifth lines contribute to the relaxation broadening of the Mossbauer peak. When $R_L >> C_L A_{M_g M_e}$ and $R_T >> C_T B_{M_g M_e}$, the contributions of the fourth and fifth lines of Eq.(14) to the line–width can be neglected. In this case, the Mössbauer peak has the Lorentzian line-shape with a width $\Gamma_{M_g M_e} + C_L A_{M_g M_e}/R_L + C_T B_{M_g M_e}/R_T$. Except for the additional transverse relaxation broadening $C_T B_{M_g M_e}/R_T$ this result agrees with that of Wegener[17] if his correlation function $< h(t)\ h\ (0) >$ has been written in the form of Eq.(13).

The overall Mossbauer relaxation line-shape of a ferric ion thus depends on the following quantities:

(a) The half-width $\Gamma_{M_g M_e}$'s and relative intensities of the three pairs of Mossbauer lines in the absence of relaxation effects.

(b) The hyperfine constants.

(c) The Boltzmann factor $p = \exp(-g\mu_B H_{eff}/K_B T)$ of successive ionic Zeeman levels. Here μ_B and H_{eff} represent Bohr magneton and the effective field acting at Fe^{3+}. The quantity p enables us to calculate $< S_z >$, $< (\delta S_z)^2 >$ and $< S_x^2 >$.

(d) The relaxation rates R_L and R_T.

The perturbative lineshape functions have been used to fit the experimental spectra by Bradford and Marshall for haemoglobin cyanides[14] and by us for Ni-Zn ferrites[7,19] and Y-AI garnets.'* The agreements between experimental spectra and the theoretical curves were observed to be very satisfactory. For these mixed ferrites and garnets, we determined the temperature dependences of the relaxation rates for ferric ions, especially, in the region of the critical temperature. It seems to us that the perturbative lineshape function, Eq.(14),

is more suitable than the stochastic one, Eq.(6), to fit the experimentally observed relaxation spectra of ferric oxides. An illustration is given in Fig. 1.

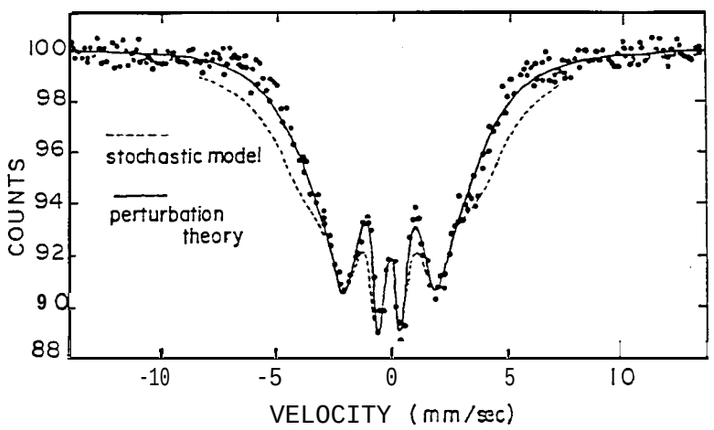

FIG. 1 The best single-site fits to the spectrum of $(Zn)_{0.20}$ (Ni), $_{80}Fe_2O_4$ at 726K.

In Fig. 1 we show the best single-site fits to the experimental spectrum of $(Zn)_{020}$ $(Ni)_{0.80}$ Fe_2O_4 at 726K $(0.955T_N)$ with Eqs.(6) and (14). In these single-site fittings, the chemical surroundings of the ferric ions in tetrahedral and octahedral sites were considered to be identical. As indicated by this figure, the goodness of fitting by the perturbative lineshape function is better than that by the stochastic one. The stochastic lineshape agrees qualitatively, not quantitively, with the experimentally observed relaxation spectrum. Thre are quite large deviations in the outer parts of the spectrum. Actually, similar difficulties were encountered in the cases of K_2FeO_4,[8] Co-Zn ferrites,[12] and Ni-Zn ferrites[6,20] when the stochastic model was used. Therefore the perturbative lineshape, rather than the stochastic one, was used to explain the experimental spectra and to extract the relaxation parameters in our work.

III. $NiFe_2O_4$ and $(Zn)_{0.10}(Ni)_{0.90}Fe_2O_4$

In the Mössbauer–effect study of the Ni-Zn ferrite system $(Zn)_x$ (Ni), $_{-x}Fe_2O_4$ with low zinc-content, say $x \leqslant 0.20$, it was found that the single-site fits to the experimental spectra with the perturbative lineshape function Eq.(14) are satisfactory enough (refer to Fig. 1). We will discuss in the following paragraphs the relaxation rate obtained from the single-site fitting for the samples $NiFe_2O_4$ and $(Zn)_{010}(Ni)_{090}Fe_2O_4$.

In our single site-fitting of these two samples, the chemical surrounding of the tetrahedral A-site ferric ion and that of the octahedral B-site ferric ion are considered to be the same. The hyperfine constants were derived from the measured hyperfine fields of a B–site ferric ion at low temperatures (down to 12 K). The half width $\Gamma_{M_gM_e}$ was obtained

from the linewidth measurement for the sample at temperatures well above T_N and was assumed to be the same for all the 6 peaks. The transverse relaxation rate R_T was assumed to be a large constant (- 1 0^{12} sec^{-1}) comparable to the spin wave frequency. The important free parameters were therefore reduced to four, i.e. the longitudinal relaxation rate R_L, the Boltzmann factor p, the isomer shift δ, and the quadrupole splitting 2ϵ.

In Fig. 2 we show the temperature dependences of the longitudinal relaxation rate R_L for the samples $NiFe_2O_4$ and $(Zn)_{0.1}(Ni)_{0.9}Fe_2O_4$. For each of the two samples we

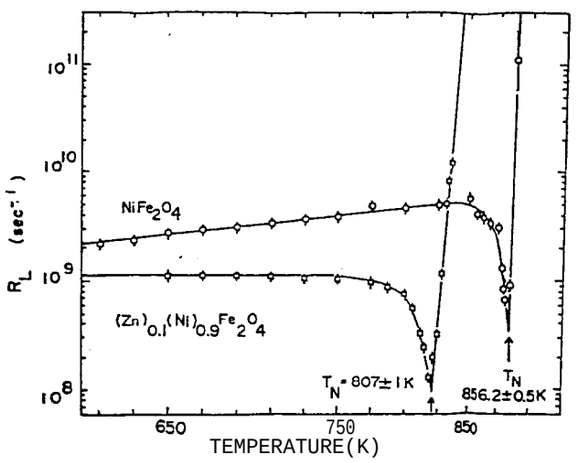

$NiFe_2O_4$ and $(Zn)_{0.10}(Ni)_{0.90}Fe_2O_4$.

also indicate the N'e T_N determined from the temperature-dependence of $< S_z >$ calculated from the Boltzmann factor p. When the temperature T is well below T_N, R_L is almost independent of T. However, when T approaches T_N and goes into the critical region, R_L decreases anomalously and then reaches a minimum at T_N. After passing through T_N, R_L increases sharply and finally diverges. We believe that the anomalous decreasing of the relaxation rate is the critical slowing-down which has often been discussed in many studies of dynamical critical–phenomena.[21]

It is generally believed that spin patches with dimensions much larger than the crystal unit cell are formed when the temperature is in the critical region. Within each patch the spins are correlated and a finite number of spins are aligned. The exchange interaction acts basically between neighboring ions while the thermal disturbance flips the spins uncorrelatively and incoherently. Thus it requires a long time to generate, destroy, or to flip a large spin patch. When the temperature approaches the critical temperature T_N of the sample, both the number and the size of the spin patches increase and therefore the relaxation time increases sharply. In other words, the relaxation rate decreases in the critical region because the spin-spin correlation length ξ increases sharply as T approaches T_N.

According to the dynamic scaling hypothesis the relaxation time τ of the long wave length modes of spin fluctuation is written as:

$$\tau \sim \xi^{z} \tag{15}$$

where the exponent z is a number slightly less than two.[22] The critical behavior of ξ is generally written as[23]

$$\xi \sim \xi_{o}(1-T/T_{N})^{-\nu'} \tag{16}$$

when T approaches T_N from below. The critical exponent ν' is equal to 1/2 for the classical model, equal to 1 for the two–dimensional Ising model, and is determined experimentally to be 0.57 for X_e.[23] From Eqs. (15) and (16) we have

$$\tau \sim (1-T/T_{N})^{-\nu' z} \tag{17}$$

If the molecular field approximation is used in the Glauber model to solve the spin relaxation time, the critical exponent $\nu' z$ in Eq.(17) equals one.[23] The same result is also predicted with van Hove 's theory.[22] In Fig. 3 we show the log–log plot of the relaxation rate as a function $1-T/T_N$ for our samples $NiFe_2O_4$ and $(Zn)_{0.1}(Ni)_{0.9}Fe_2O_4$. The critical exponents of the relaxation rates obtained from this plot are

$$\begin{aligned} \nu' z &= 0.9 \pm 0.1 \qquad x = 0.0 \\ &= 0.91 \pm 0.03 \qquad x = 0.1 \end{aligned} \tag{18}$$

which are near to unity.

In Fig.(2) we also noted that the critical slowing down for the x = 0.0 sample is narrower and deeper than that for the x = 0.1 sample. This feature follows from the fact that the introduction of nonmagnetic zinc ions breaks some superexchange–bonds and thus decreases the spin correlation length ξ_o at 0K. If the Gaussian approximation is used in the phase–transition model of Ginzberg and Landau, the critical range ΔT is related to ξ_o by [22]

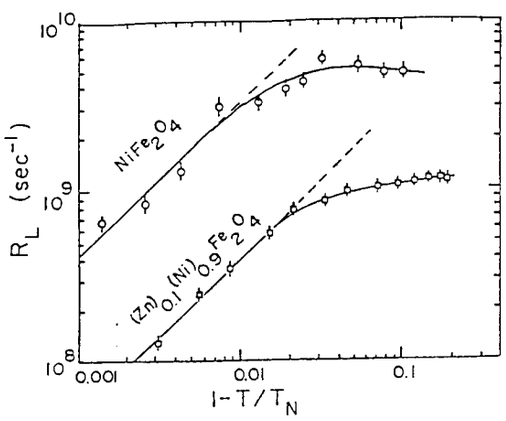

FIG. 3 The log–log plot of R_L vs $(1-T/T_N)$ for $NiFe_2O_4$ and $(Zn)_{0.10}(Ni)_{0.90}Fe_2O_4$.

$$AT \sim \xi_o^{-6} \tag{19}$$

Therefore, due to the broadening of AT the slowing down becomes less sharp when more zinc ions have replaced the nickel ions. Actually we have observed that the "critical range" becames so broad- that the critical slowing down completely disappears with zinc-content $x \geqslant 0.50$.'

JV. $Y_3 Al_{,,} Fe_{3\,5} O_{12}$

In many iron-contained magnetic materials such as ferrites and garnets, the iron atoms are distributed over non-equivalent lattice points or interstitial sites. An example[24] is the yittrium aluminum-iron garnet system $Y_3 Al_x Fe_{5-x} O_{12}$ with $0 \leqslant x \leqslant 5$. In this material ferric ions distribute over octahedral a- and tetrahedral d-sites. Each a-site ferric ion is surrounded by 6 nearest oxygen anions and 6 d-site next-nearest cations. While each d-site ferric ion is surrounded by 4 nearest oxygen anions and 4 a- and 4 d-site next–nearest cations. Since the a-0-d superexchange interaction determines the supertransferred hyperfine field at the nucleus and the effective field at the ion, the hyperfine constants and the Boltzmann factor of the a-site ferric ion are different from those of the d–site ferric ion. On the other hand, in magnetic dielectrics the most important relaxation process is the magnon–magnon scattering process in which the magnetic interaction between ions plays the dominant role. One thus expects that the relaxation rates of the a- and d-site ferric ions are also different. Hence the Mossbauer spectrum of $Y_3 Al_{,} Fe_{5-x} O_{12}$ should consists of two sub-spectra characterized by different hyperfine constants, different Boltzmann factors, different relaxation rates, different isomer shifts, and different quadrupole splittings. Therefore, the two-site fitting is expected to be necessary for the $Y_3 Al_x Fe_{5-x} O_{12}$ system.

In Fig. 4 we show as an example the Mössbauer spectrum of $Y_3 Al_{,,} Fe_{3\,5} O_{12}$ at 3 10K and its best two-sites fit with Eq.(14). This spectrum can not be fit satisfactorily with the single-site fitting. In the two-sites fittings of the spectra for this sample, the area-ratio and the hyperfine constants of the a- and d-site sub-spectra were obtained from the well-resolved spectra at low temperatures (12K) and were assumed to be independent of the temperature. The $\Gamma_{M_S M_g}$'s were obtained from the linewidth measurements at temperatures well above T_N .

The temperature dependences of the longitudinal relaxation rates R_{La} and R_{Ld} are shown in Fig. 5. In the same figure we also indicate the N'eel temperature 335±1K obtained from the temperature dependence of the Boltzmann factor p. When the temperature is low, the relaxation rates increase with temperature as expected until flat local maxima near 220K are reached. Then the relaxation rates decrease gradually over a fairly large range of temperature (AT $\sim$90K) and finally increase sharply when T_N is approached.

The slight decreases in R_{La} and R_{Ld} before. T_N is reached were recognized as the

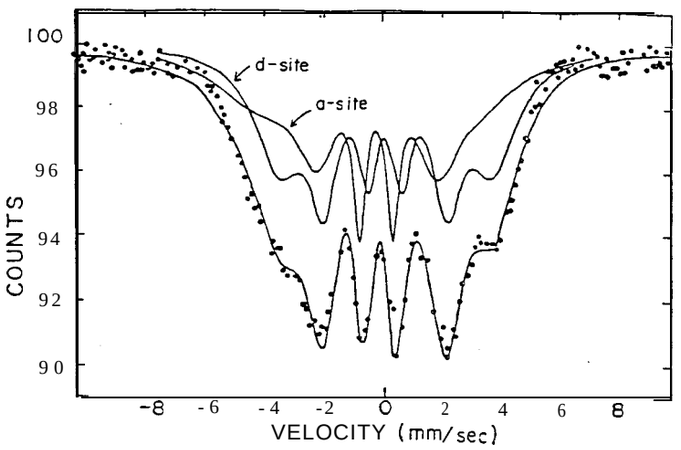

FIG. 4 The best two-sites tit to the spectrum of $Y_3 Al, _5 Fe_3 _5 O_{12}$ at 3 10K.

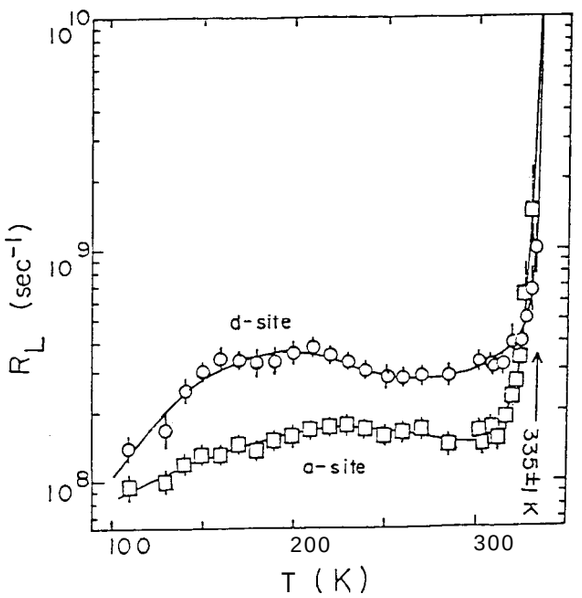

FIG. 5 The longitudinal relaxation rates of $Y_3 Al,., Fe_{3.5} O_{12}$.

blurred critical slowing-downs with a very broad critical range. As we have discussed in III, replacing the magnetic ferric ions with the non-magnetic aluminum ions reduces the correlation length ξ_0 and thus broadens the critical range of temperature.

The longitudinal relaxation in magnetic materials is caused by the thermal modulation of the magne tocrystalline aniso tropy energy. Of the three interactions which are responsible for the anisotropy energy, the single ion anisotropy arising from the effect of crystal

field can only cause the magnon-phonon scattering. The dipole-dipole interaction and the anisotropic part of the exchange interaction can cause both the magnon-magnon and magnon-phonon scatterings.

In the $Y_3Al_xFe_{5-x}O_{12}$ svstem. a d-site ferric ion has more cation neighbors then an a -site ferric ion does. The strength a_{Fe} of the interaction between the ferric ion and the crystal field for a-site ferric ions is larger than that for d-site ferric ions:[25]

$$a^a_{Fe} = 1.94 \times 10^{-2} \text{ cm-'}$$

$$a^d_{Fe} = 0.65 \times 10^{-2} \text{ cm-'} \tag{20}$$

The observation that. $R_{Ld} > R_{La}$ in the temperature range $110 < T < 325K$ indicates that the single-ion anisotropy does not play the dominant role in the longitudinal relaxation in this range.

The magon scattering processes which can contribute to the longitudinal relaxation rates are those processes in which the magnon number is changed. The lowest order processes of this kind caused by the modulations of the dipole-dipole interaction and the anisotropic part of exchange interaction are the 3− magnons process and the 2-magnons −1−phonon processes. The contributions R_3 and R_{21} of these processes to the longitudinal relaxation rate were given respectively by:[26]

$$R_3 \approx \begin{cases} 0.4\ (g^2\mu_B^2 M_0^2/2JS\hbar)(K_B T/2JS)^{1/2} \varrho_n{}^2 (g\mu_B H_{eff}/K_B T) \\ \text{when } g\mu_B H_{eff} \ll K_B T \\ 1.4(g^2\mu_B^2 M_0^2/2JS\hbar)(g\mu_B H_{eff}/2JS)^{1/2} \exp(-g\mu_B H_{eff}/K_B T) \\ \text{when } g\mu_B H_{eff} \gg K_B T, \end{cases}$$

$$R_{21} \approx \begin{cases} (g\mu_B M_0/\hbar)(g\mu_B M_0/\rho a^3 C^2)(T/\Theta_D)^3 \text{ when } T \ll \Theta_D^2/T_c \\ (\hbar/\rho a^5)(g\mu_B M_0/K_B T_C)\ (T/T,)^{"} \text{ when } T \gg \Theta_D^2/T_C. \end{cases} \tag{21}$$

for the dipole-dipole interaction. In this equation, g,M_o, J, S, H_{eff}, *p*, *a*, *C*, Θ_D, and T_c are, respectively, the g factor of the ion, the saturation magnetization, the isotropic exchange constant, the spin of the ion, the effective magnetic field acting at the ion, the mass density of the sample, the lattice constant, the sound velocity, the Debye temperature, and the curie or the Ne'el temperature. For the anisotropic part of the exchange interaction, the contributions to the relaxation rate of these magnon processes are expected to have

the same forms as Eq. (21). A very interesting feature in Eq. (2 1) is that $R_3^{'}$ diverges when the temperature approaches the critical temperature at which H_{eff} vanishes, whereas R_{21} remains finite for all temperature. Since we have observed in Fig. 5 the divergence of R_L's at T_N. We know that the magnon-magnon processes are the main processes when the temperature is not very low.

V. $Na_2O \cdot 5.5\ (Fe_{0.5}Al_{0.5})_2O_3$

The Mossbauer spectra of the iron-doped β''–alumina with composition $Na_2O \cdot 5.5\ (Fe_{0.5})_2O_3$ were taken at various temperatures from 13.4 to 790K. The representative spectra are shown in Fig. 6. At low temperatures, the spectra consist of well-resolved Zeeman patterns. This means that all ions are magnetically ordered. When the temperature raises to about 40K, a paramagnetic quadrupole doublet appears and superimposes on the well resolved six-lines Zeeman pattern. This means that a considerable amount of iron ions are now in the paramagnetic state while the others are still in a magnetically ordered state. The paramagnetic ions and magnetic ions continue to coexist when the temperature rises to 300K. At 300K the subspectrum corresponding to the ordered ions becomes a very broad "Y" superimposing on the paramagnetic quadrupole doublet. This sub-spectrum disappears completely at T = 410 ± 20K.

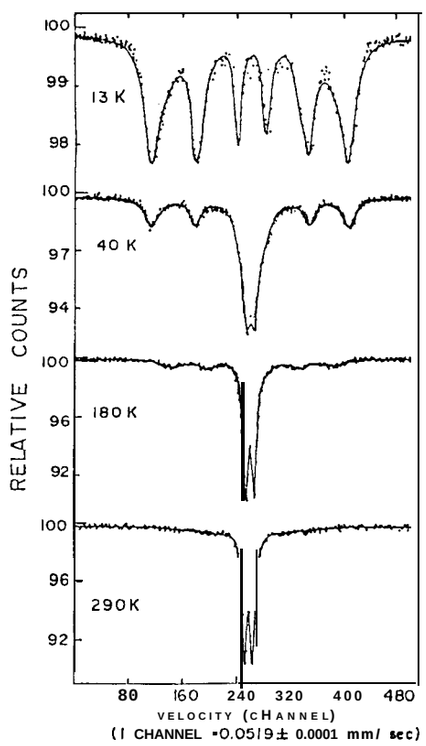

FIG. 6 Representative Mossbauer Spectra of the iron doped β''-alumina Na, 0.55 $(Fe_{0.5}(Al_{0.5})_2O_3$. The solid curres are the best fits.

The magnetically ordered ions were identified to be ferric ions in tetrahedral sites from the measurement of the hyperfine field at low temperatures. The para-magnetic ions were identified to be ferric ions in the octahedral sites from the measurements of quadrupole splitting at high temperatures. The spectra taken at T > 40K were then fitted with a relaxation-broadened Zeeman pattern superimposing on a quadupole doublet.. For spectra taken at $T < 40K$, the two-sites fitting described in IV were used. A typical tit is given in Fig. 7.

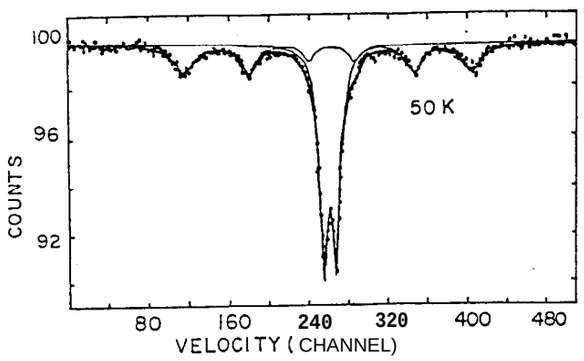

FIG. 7 Best fit to-the spectrum of $Na_2O{\cdot}5.5(Fe_{0.5}Al_{0.5})_2O_3$ at 50K.

In Fig. 8 we show the temperature dependence of the longitudinal relaxation rate for the ferric ions in tetrahedral sites in the temperature range $13.4 \leqslant T \leqslant 290K$. When T < 260K, the relaxation rate increases proportionally to the temperature with a slope of (8.0 ± 0.3) x $10^5 sec^{-1} K^{-1}$. The proportional dependence on T of the longitudinal relaxation rate can easily be recognized to be due to the direct process of spin lattice relaxation in which a transition in the spin system is accompanied with a creation or anihilation of a phonon. However, the detailed relaxation mechanism for this "superionic conductor" containing sodium ions is not known and some more studies are needed.

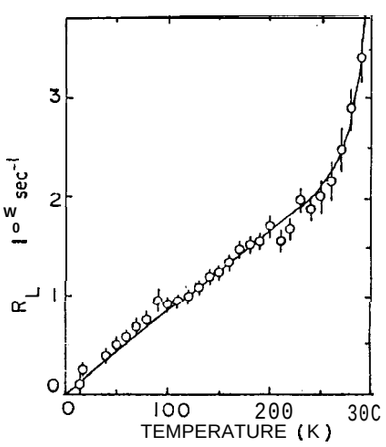

FIG. 8 Temperature dependence of the relaxation rate for $Na_2O{\cdot}5.5(Fe_{0.5}Al_{.5})_2O_3$.

REFERENCES

1. For example: J. Gal., Z. Hadari, and U. Atzmony, E.R. Bauminger, I. Nowik, and S.Ofer, Phys. Rev. B8, 1901 (1982).
2. For example: (a) CL. Chien, Phys. Rev. B18, 1901(1973). (b) P.K. Tseng, S.Y. Chuang, and H.S. Chen, J. Appl. Phys. 50, 4292(1979). (c) H.N. Ok and A. H. Menish, Phys. Rev. B22, 3471(1980).
3. L.M. Levinson, M Luban, and S. Strikman, Phys. Rev. 177, 864(1969).
4. H. Yamamoto, T. Okada, H. Watanabe and M. Fukase, J. Phys. Soc. Japan 24, 275 (1968).
5. 1. Nowik and H.H. Wickman, Phys, Rev. Lett. 31, 949(1966).
6. S.C. Bhargava and P.K. lyengar, J. Phys. 35, C6–669(1974).
7. T.M. Uen and P.K. Tseng, Phys. Rev. B25,1848(1982).
8. G.R. Hoy and M.R. Corson, in Mössbauer Spectroscopy and Its Chemical Applications edited by J.F. Stevens and G.K. Shenoy (American Chemical Society, Washington, D.C., 1981) P. 463.
9. For example, A.J. Dekker, in Hyperfmd Interactions edited by A.J. Freeman and R.B. Frankel (Academic Press, New York, 1967) Chapter S6.
10. M.J. Clauser and M. Blume, Phys. Rev. B3, 593(1971).
11. For example: (a) H.H. Wickman and C.F. Wagner, J. Chem. Phys. 51, 435(1969). (b) F. Sontheimer, D.L. Nagg, I. Dezsi, T. Lohner, G. Ritter, D. Seyboth, and H. Wegener, J. Phys. C6, C6–443(1974).
12. S.C. Bhargava and P.K. Iyengar, Phys. Stat. Sol. 653, 359 (1972).
13. S.C. Bhargara and N.Zeman, Phys. Rev. B21, 17 17 (1980).
14. E. Bradford and W.M. Marshall, Proc. Phys. Soc. (London) 87, 731(1966).
15. L.M. Levinson and M. Luban. Phys. Rev. 172, 268(1968).
16. L.D. Landau and E.M. Lifshitz, Statistical Physics (English translation, Addison–Wesley, London, 1974) Chapter 12.
17. H. Wegener, Z. Phys. 186,498 (1965).
18. T.M. Uen, D.E. Chen, C.C. Dai, and P.K. Tseng, J. Magn. Magn. Mat. 31-34, 789 (1983).
19. T.M. Uen and P.K. Tseng. J. Phys. 40, C2–261(1979).
20. T.M. Uen and P.K. Tseng, in Research Reports 1975 (Physics Research Center, NSC, ROC) P. 615.
21. For example, P.C. Hohenberg and B.I. Halperin, Rev. Mod. Phys. 49,435 (1977).
22. S.K. Ma, Modem Theory of Phase Transitions (Benjamin INC., New York, 1976) P.8, P.94, P.447.
23. H.E. Stanley, Introduction to Phase Transition and Critical Phenomena (Oxford University Press, New York, 197 1) P. 45-47, P. 280.
24. C.W. Chen, Magnetism and Metallurgy of Soft Magnetic Materials (North Holland Pub. Co., New York, 1977) P. 212-215.
25. G.P. Rodrigue, H.M. Meyer, and R.V. Jones, J. Appl Phys. 31, 376S(1960).
26. M.I. Kaganov and V.M. Tsukemik, Sov. Phys. JETP 7, 1107 (1958).